

3-D Photoionization Structure and Distances of Planetary Nebulae III. NGC 6781

Hugo E. Schwarz¹, Hektor Monteiro^{1,2}

1 Cerro Tololo Inter-American Observatory¹, Casilla 603, Colina El Pino S/N, La Serena, Chile

2 Department of Physics and Astronomy, Georgia State University, 1, Park Place South, Atlanta, GA 30302, USA

ABSTRACT

Continuing our series of papers on the three-dimensional (3-D) structures of and accurate distances to Planetary Nebulae (PNe), we present our study of the planetary nebula NGC 6781. For this object we construct a 3-D photoionization model and, using the constraints provided by observational data from the literature we determine the detailed 3-D structure of the nebula, the physical parameters of the ionizing source and the first precise distance. The procedure consists in simultaneously fitting all the observed emission line morphologies, integrated intensities and the 2-D density map from the [SII] line ratios to the parameters generated by the model, and in an iterative way obtain the best fit for the central star parameters and the distance to NGC 6781, obtaining values of 950 ± 143 pc and $385 L_{\odot}$ for the distance and luminosity of the central star respectively. Using theoretical evolutionary tracks of intermediate and low mass stars, we derive the mass of the central star of NGC 6781 and its progenitor to be $0.60 \pm 0.03 M_{\odot}$ and $1.5 \pm 0.5 M_{\odot}$ respectively.

Subject headings: Planetary Nebula – Interstellar medium – photoionization modeling

1. Introduction

Planetary nebulae are the end products of the evolution of stars with masses below about $8M_{\odot}$ (Pottasch (1984) and Iben & Renzini (1983)). The importance of these objects

¹Cerro Tololo Inter-American Observatory, National Optical Astronomy Observatory, operated by the Association of Universities for Research in Astronomy, Inc., under a cooperative agreement with the National Science Foundation.

extends beyond the understanding of how the outer layers of stars end up forming the many observed morphologies. Indeed, PNe have been used for many purposes, from understanding basic atomic and plasma processes (Aller (1987)) to determining chemical evolution of our Galaxy (Maciel & Costa (2003)). Recently PNe are also being used to study galaxies other than our own, providing powerful tools to determine distances, kinematics and chemical properties of external galaxies (Ciardullo (2003)) and even to trace inter-cluster material as in Feldmeier et al. (2004). PNe have the advantage that they are observable out to large distances due to their luminous narrow emission lines, especially [OIII]500.7nm, being useful also as standard candles through the use of the PN luminosity function (for extensive discussion see Jacoby et al. (1999)).

One of the most important problems in observational Galactic PNe research is the difficulty in determining their distances and three-dimensional structures. Observations always produce a 2-D projection of their 3-D structure, and recovering the original structure is not trivial. This is also made worse by the fact that only crude distances, usually obtained from statistical methods on large samples, can be determined. Large uncertainties are generated by the need to assume constancy of one parameter such as the nebular size, (ionized) mass, flux etc. so that typical errors in the distances to individual objects are of the order of a factor of 3 or more. Very few nebulae have had individual accurate distances determined.

Historically, PNe have been studied with empirical methods and one dimensional photoionization models, leading to the above mentioned problems. In contrast to this, our technique developed and described in Monteiro, Schwarz, Gruenwald & Heathcote (2004) provides precise, self-consistently determined distances, as well as the physical parameters for the central star and gaseous nebula, for objects with sufficient observational constraints. These objects can provide valuable calibration for existing distance scales as well as self-consistently determined physical and chemical quantities. For a detailed description of our novel method see our previously published papers in this series and especially the extensive explanatory appendix in the second paper Monteiro, Schwarz, Gruenwald, Guenther & Heathcote (2005).

In this work we focus on the PN NGC 6781 (RA $19^h 18^m 28^s$ Dec. $+06^\circ 32' 19''$ 2000.) shown in Figure 1. This is a PN whose main structure is observed as a 130" diameter bright shell of low ellipticity, double in parts and with fainter lobes emanating at the N-S ends where the ring is double and fainter. The ring is brighter in the E-W directions as also shown in Figure 1 of Mavromatakis et al. (2001). Their image is available as a fits file on the web at <http://www.ing.iac.es/rcorradi> and our Figure 1 has been produced using this image.

Mavromatakis et al. (2001) claim a possible faint halo extending out to about 3' by

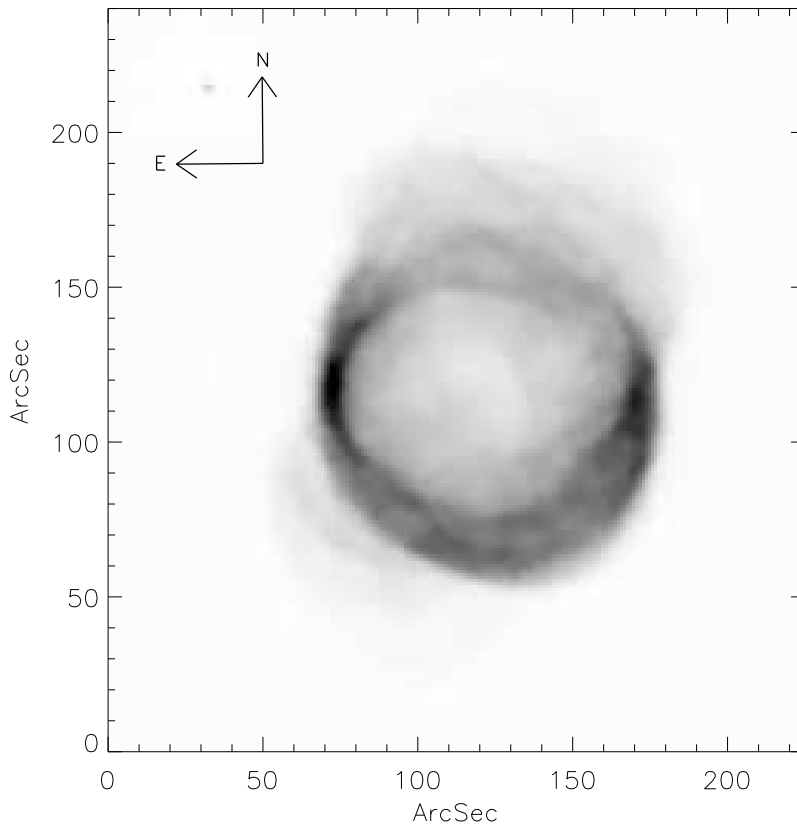


Fig. 1.— Narrowband image of NGC 6781 in the light of the [NII]658.4nm line. Image produced from the original of Mavromatakis et al. (2001).

4' surrounding NGC 6781. Note that Corradi et al. (2003) list the object in their paper on the search for faint haloes around bright PNe, but do not make any statement about having detected a halo according to their criteria, which include the candidate halo having to be limb brightened and/or detached. The halo of Mavromatakis et al. (2001) is not limb brightened and more likely to be the result of scattered light in the instrument.

For a more detailed discussion of the morphology of NGC 6781 based on a set of narrow band images, as well as density, temperature, and extinction maps see Mavromatakis et al. (2001).

An estimate for the luminosity, temperature, and mass of the CS of NGC 6781 based on statistical analysis is $127 L_{\odot}$, 105 kK, and $0.6 M_{\odot}$, respectively, taken from Stanghellini, Villaver, Manchado & Guerrero (2002). The average distance of the 12 literature values we found in Acker et al. (1992) is 946 pc with the individual values ranging from 500 to

1600 pc, a factor of more than three.

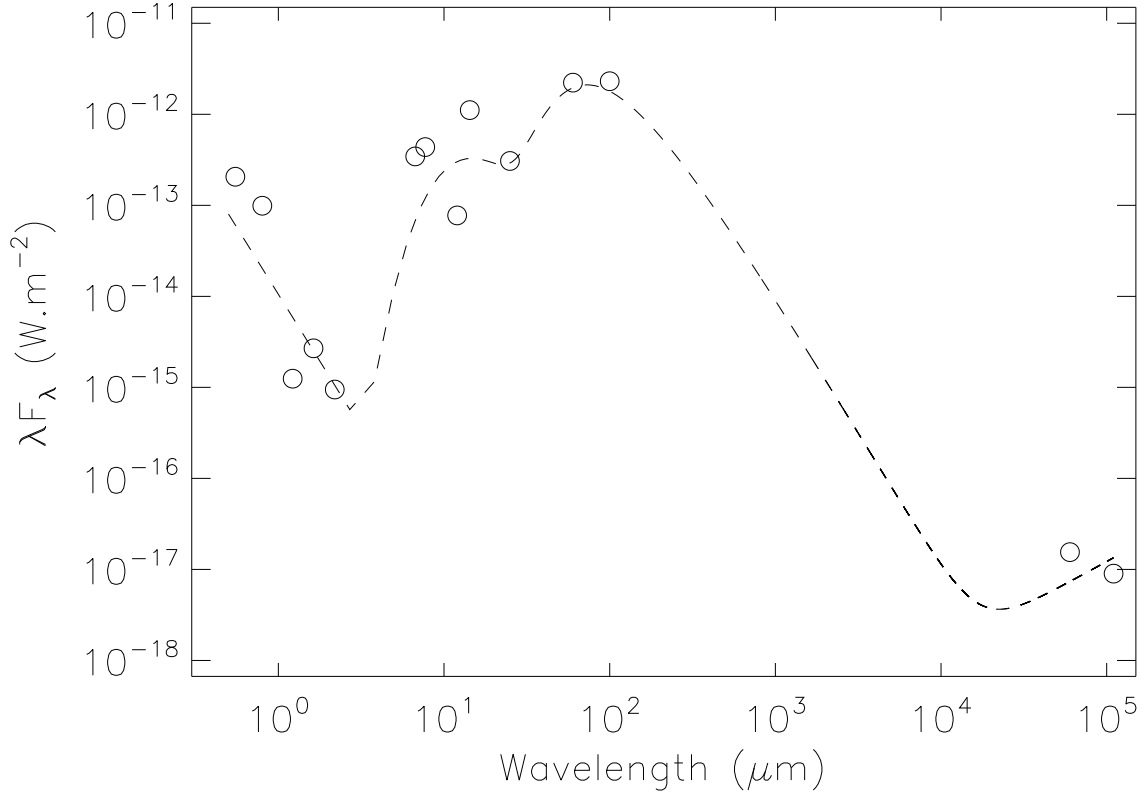


Fig. 2.— The graph shows the Spectral Energy Distribution (SED) of NGC 6781 over more than five decades of wavelength interval. All values were obtained from the literature. The dotted curve is a combined blackbody and continuum radiation fit to the data.

The Spectral Energy Distribution (SED) $\lambda F(\lambda)$ of NGC 6781 shows a broad blackbody-like spectrum between about 1 and 100 μm , a radio tail out to 12 cm, and a rise toward the blue which probably comes from the hot central star. Integrating the $F(\lambda)$ curve we obtain a luminosity of $L = 166 \text{ d}^2 (\text{kpc}) L_{\odot}$. The luminosity of NGC 6781 is therefore $150 L_{\odot}$ at its distance of 950 pc. Applying the usual correction according to Myers et al. (1987) we obtain $L = 225 L_{\odot}$.

Here we present our own modeling results using observational data published in the literature as constraints and derive the 3-D structure, chemical abundances, CS properties, and distance for NGC 6781 in a self-consistent manner.

In §2 we discuss the observational data used as constraints for the models. In §3 we

present the model results generated by the 3-D photoionization code, and we discuss the derived quantities. In §4 we give our overall conclusions and discuss possible discrepancies with other determinations of parameters for this nebula.

2. Observations

The observational data that we used to constrain our model for NGC 6781 were taken from the literature. Mavromatakis et al. (2001) presents narrow band imaging of the nebula in the most important lines such as $H\alpha$, $H\beta$, [OIII] and others. He also provides [SII] narrow band images to obtain a spatially resolved density map, as well as the $H\alpha/H\beta$ extinction map of the nebula. We used their 2-D density map to infer the 3-D density structure to be used as an input for the photoionization model.

Liu, Liu, Luo & Barlow (2004) present deep optical spectra of medium resolution for NGC 6781 and 11 other planetary nebulae. The observations were carried out with a long-slit spectrograph covering from 360 to 800 nm and include all important emission lines. Their observations are particularly interesting because the objects were scanned with the long-slit across the nebular surface by driving the telescope differentially in right ascension. These observations then yield average spectra for the whole nebula, which are in principle more precise than single slit observations, and allow us to produce emission line maps of the object. For details of the observations and their reduction procedure as well as the full tables of line fluxes, see Liu, Liu, Luo & Barlow (2004). The most important lines used as constraints for the model are listed in our Table 1 together with the corresponding values from our model.

We also used the $H\alpha + [\text{NII}]$ image from Mavromatakis et al. (2001) to determine the size of NGC 6781 thus using it as one of the constraints for the distance obtained in our model calculations.

3. Photoionization Models for NGC 6781

The photoionization code we used for the study of NGC 6781 is the Mocassin code described in full detail in Ercolano et al. (2003). This code allows for the same possibilities as the code used previously in Monteiro, Morisset, Gruenwald & Viegas (2000) but is more sophisticated in that the diffuse radiation is fully taken into account in an efficient manner. The previous code also had this ability but the associated increase in computational time was prohibitive.

The basic procedure adopted to study NGC 6781 is the same, independent of the code

and has been fully described in the two previous papers in this series (Monteiro, Schwarz, Gruenwald & Heathcote (2004) and (especially the appendix of) Monteiro, Schwarz, Gruenwald, Guenthner & Heathcote (2005)). In short, we gather as much observational material as possible and use it to constrain our model with many data simultaneously. Of particular interest are the total line fluxes and line images corrected for reddening, and the line diagnostic ratio maps. The structure adopted for the nebulae is defined based on the observed density map, when available, or density profiles from single slit observations plus the observed projected morphology in several emission lines.

In the case of NGC 6781 in particular, the initial structure was based on density maps published by Mavromatakis et al. (2001). It is clear from the images and density map (from the [SII] doublet ratio) presented here, that the density is lower in the central region than in the main bright ring. This indicates that the structure must have lower density material in the line of sight of those regions and therefore the best structure to reproduce the observed projected morphology is an open ended structure or hour-glass shape, which we therefore adopt for this object. It is also clear from the images in many narrow band filters that the material is highly clumpy, so to reproduce this we include random density fluctuations in the adopted structure. The final adopted structure in its best fitting orientation on the sky is presented in Figure 3.

4. Model Results

We present here the main results obtained from the photoionization model constrained by the observational data. The integrated fluxes for 12 emission lines are given in Table 1, as well as the fitted abundances and ionizing star parameters.

The model fitting procedure which uses the model image size fitted to the observed one for the line [NII]658.4nm, as well as the absolute $H\beta$ flux, and the integrated fluxes of all other lines gives a distance of 950 ± 145 pc for NGC 6781. The error on this distance has been computed in the same way as in our previous papers in this series.

In Fig. 4 we show the projected images obtained from the fitted model. Notice that all major morphological features of the object are well reproduced as well as the general ionization stratification in the different emission lines. In particular the images for [OIII] 500.7 and HeII 468.6 show very good agreement with those obtained by Mavromatakis et al. (2001) as well as the more common [NII] 658.4 nm and $H\alpha$.

Figure 5 shows the final model image for [NII] 658.4 nm plotted in contours over the observed image by Mavromatakis et al. (2001). Again the good agreement of the apparent

size, obtained from the size of the fitted model grid and our determined distance, is evident.

As with objects studied in previous works, the mass of the ionizing star, as well as its progenitor and age are determined from theoretical cooling tracks. Here we have used the cooling tracks of Vassiliadis & Wood (1994) because their grids present a good (= close) sampling of progenitor masses in the 1 to $3M_{\odot}$ range. In Figure 6 we show the position of NGC 6781, as well as the other objects that we have studied previously with this method, along with the theoretical cooling tracks. From this we obtain the mass of the central star of and its progenitor to be $0.60 \pm 0.03 M_{\odot}$ and $1.5 \pm 0.5 M_{\odot}$ respectively. Figure 6 also shows the position of these same objects as determined by different authors by distinct techniques. All PNe central stars are well evolved on their cooling track except NGC 6369.

5. Discussion and conclusions

As with all our other PNe central star temperatures determined by this 3-D structure method we generally find higher temperatures than those computed from oxygen lines and nearer those from HeII lines. Table 2 shows a comparison of parameters from the literature and those determined by us in this and previous papers.

Note that Phillips (2003) found that bipolar PNe have average $T(\text{HeII}) = 138\text{k}$; ellipticals 92k ; round 81k whole sample 87k . This was also found earlier by Corradi & Schwarz (1995) who determined $T(\text{bipolars}) = 142\text{k}$; irregulars 99k ; ellipticals 76k ; and unresolved 63k . This general trend is always observed, and our high temperature for bipolar NGC 6781 is no exception.

The central star properties of all PNe that we have applied our method to are shown in the HR diagram of Figure 6. Also shown are the values determined by other methods, taken from the literature. There are large differences between our values and those previously published for NGC 6781 and NGC 6369 and in both cases the central star luminosity determined by our method was higher than the literature value. This is because it was assumed that these nebulae are radiation bound but we have shown them to be matter bound as they lose up to 70% of their UV radiation to space, resulting in an underestimation of both the luminosity and temperature. The blue rise in the SED for NGC 6781 also confirms that blue radiation is escaping from the nebula. Note that the central star luminosity from our model, $L = 385 / L_{\odot}$ is larger than the luminosity derived from the observed SED $L = 225 / L_{\odot}$ by a factor of 1.7, confirming that the nebula is matter bound and that a significant fraction of the stellar UV flux escapes from the object.

We claim that ours are the most accurate luminosities and temperatures that have been

determined for these stars to date. Interestingly our values tend to bring the core masses closer to $0.6 M_{\odot}$ which is also the peak value of the narrow mass distribution of white dwarfs.

We acknowledge the continuing support of NOAO’s Science Fund to HM and the generous hospitality of the Nordic Optical Telescope on La Palma.

REFERENCES

- Acker, A., Ochsenbein, F., Stenholm, B., Tylanda, R., Marcout, J., Schohn, C. 1992, Strabourg-ESO Catalogue of Galactic PNe.
- Aller, L.H. Physics of Thermal Gaseous Nebulae, Reidel.
- Blöcker, T. 1995, A&A, 299, 755
- Cahn, J.H., Kaler, J.B.; & Stanghellini, L. 1992, A&AS, 94, 399
- Ciardullo, R. 2003, Lecture Notes in Physics, 635, 243
- Corradi, R.L.M., Schönberner, D., Steffen, M., Perinotto, M. 2003, MNRAS, 340, 417
- Corradi, R.L.M., Schwarz, H.E. 1995, A&A, 293, 871
- Ercolano, B., Barlow, M. J., Storey, P. J., & Liu, X.-W. 2003, MNRAS, 340, 1136
- Feldmeier, J.J., Ciardullo, R., Jacoby, G.H., Durrell, P.R. 2004, ApJ, 615, 196
- Filippenko, A. V. 1982, PASP, 94, 715
- Gruenwald, R., Viegas, S. M., & Broguière, D. 1997, ApJ, 480, 283
- Gurzadyan, G.A. 1997 “The Physics and Dynamics of Planetary Nebulae”, Springer
- Huggins, P.J., Bachiller, R., Cox, P., Forveille, T. 1996, A&A, 315, 284
- Iben, I., & Renzini, A. 1983, ARA&A, 21, 271
- Jacoby, G. H., Ciardullo, R., & Feldmeier, J. J. 1999, ASP Conf. Ser. 167: Harmonizing Cosmic Distance Scales in a Post-HIPPARCOS Era, 167, 175
- Kaler, J.B., Jacoby, G.H. 1989 AJ 345, 871
- Kaler, J.B., Shaw, R.A., Browning, L. 1997, PASP, 109, 289

- Liu, Y., Liu, X.-W., Luo, S.-G., Barlow, M. J. 2004, MNRAS 353, 1231
- Maciel, W.J., Costa, R.D.D. 2003 IAUS 209, 551 Eds. Kwok et al.
- Marston, A.P., Bryce, M., López, J.A., Palmer, J.W., Meaburn, J. 1998, A&A, 329, 683
- Mavromatakis, F., Papamastorakis, J., Paleogolou, E.V. 2001, A&A, 280, 287
- McCall, M. L. 1984, MNRAS, 208, 253
- Monteiro, H., Morisset, C., Gruenwald, R., & Viegas, S. M. 2000, ApJ, 537, 853
- Monteiro, H., Gruenwald, R., Morisset, C., & Viegas, S. M. 2002, Revista Mexicana de Astronomia y Astrofisica Conference Series, 12, 170
- Monteiro, H., Schwarz, H.E., Gruenwald, R., & Heathcote, S.R. 2004, ApJ, 609, 194
- Monteiro, H., Schwarz, H.E., Gruenwald, R., Guenthner, K., & Heathcote, S.R. 2005, ApJ, 620, 321
- Myers, P. C.; Fuller, Gary A.; Mathieu, R. D.; Beichman, C. A.; Benson, P. J.; Schild, R. E.; Emerson, J. P. 1987, ApJ, 319, 340
- Osterbrock, D. E. 1989, Research supported by the University of California, John Simon Guggenheim Memorial Foundation, University of Minnesota, et al. Mill Valley, CA, University Science Books
- Perek, L. 1971, Bull.Astr.Inst.Cz., 22, 103
- Phillips, J.P. 2003, MNRAS 344, 501
- Pottasch, S.R. 1984, Planetary Nebulae, Reidel
- Rauch, T., Deetjen, J. L., Dreizler, S. e Werner, K. 2000, Asymmetrical Planetary Nebulae II: From origins to microstructures, ASP Conference Series 199, 337
- Rice, M., Schwarz, H.E., Monteiro, H. 2004 AAS Abs. 20513813
- Schwarz, H. E., Corradi, R. L. M., & Melnick, J. 1992, AApS, 96, 23
- Schwarz, H. E., Aspin, C., Corradi, R. L. M., Reipurth, B. 1997, A&A, 319, 267
- Seaton, M. J. 1979, MNRAS, 187, 73
- Stanghellini, L., Corradi, R.L.M., Schwarz, H.E. 1993, A&A, 279, 521

- Stanghellini, L., Villaver, E., Manchado, A., & Guerrero, M. A. 2002, *ApJ*, 576, 285
- Van de Steene, G.C., Zijlstra, A.A., 1995, *A&A*, 293, 541
- Vassiliadis, E., Wood, P.R. 1994, *ApJS*, 92, 125
- Webster, B. L.; Payne, P. W.; Storey, J. W. V.; Dopita, M. A. 1988, *MNRAS*, 235, 533
- Zhang, C. Y. 1995, *ApJS*, 98, 659

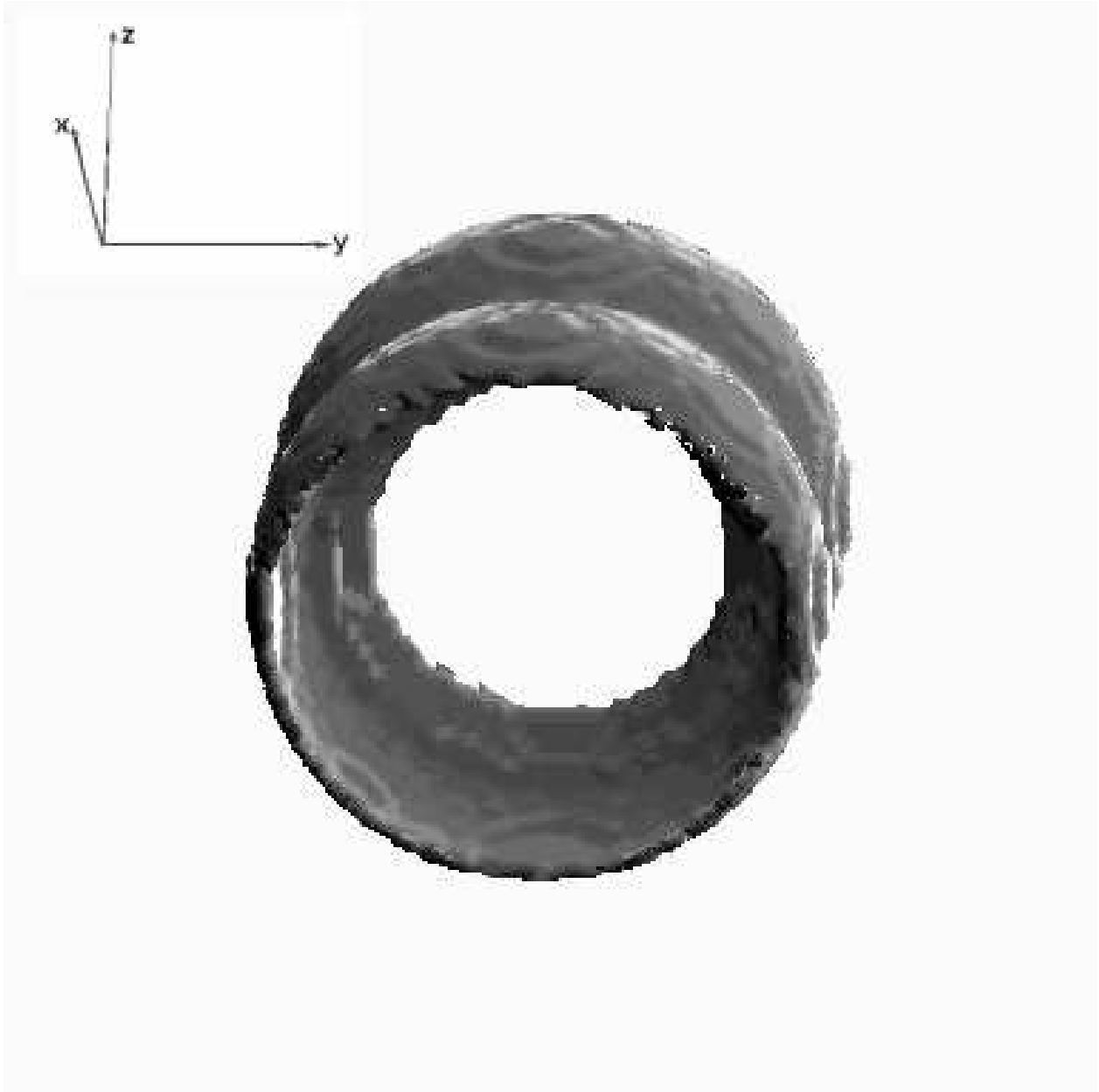


Fig. 3.— The image shows an isodensity surface of the structure adopted for NGC 6781 in its final fitted spatial orientation indicated in the upper left hand corner.

Table 1: Observed and model line fluxes and model central star parameters for NGC 6781.

	Observed	Model	Rel. Error
T_* (K)	-	123kK	-
L_*/L_\odot	-	385	-
$\log(g_*)$	-	7.0	-
Distance (pc)	500-1600	950	± 0.143
Density	100-1400	100-1400	-
He/H	-	1.25×10^{-1}	-
C/H	-	5.95×10^{-4}	-
N/H	-	9.75×10^{-5}	-
O/H	-	3.50×10^{-4}	-
Ne/H	-	7.10×10^{-5}	-
Ar/H	-	2.26×10^{-6}	-
S/H	-	0.28×10^{-5}	-
$\log(H\beta)$	-9.80	-9.84	-0.09
[NeIII] 386.8 ^a	1.09	1.06	-0.03
[OIII] 436.3	0.05	0.07	0.28
HeII 468.6	0.09	0.09	0.02
[OIII] 500.7	8.23	7.10	-0.14
[NII] 575.5	0.07	0.07	0.07
HeI 587.6	0.16	0.17	0.09
[OI] 630.2	0.33	0.38	0.15
H α 656.3	2.65	2.86	0.08
[NII] 658.4	3.96	3.88	-0.02
[SII] 671.7	0.25	0.25	-0.01
[SII] 673.1	0.21	0.21	0.00

a) Value obtained by Kaler, Shaw & Browning (1997)

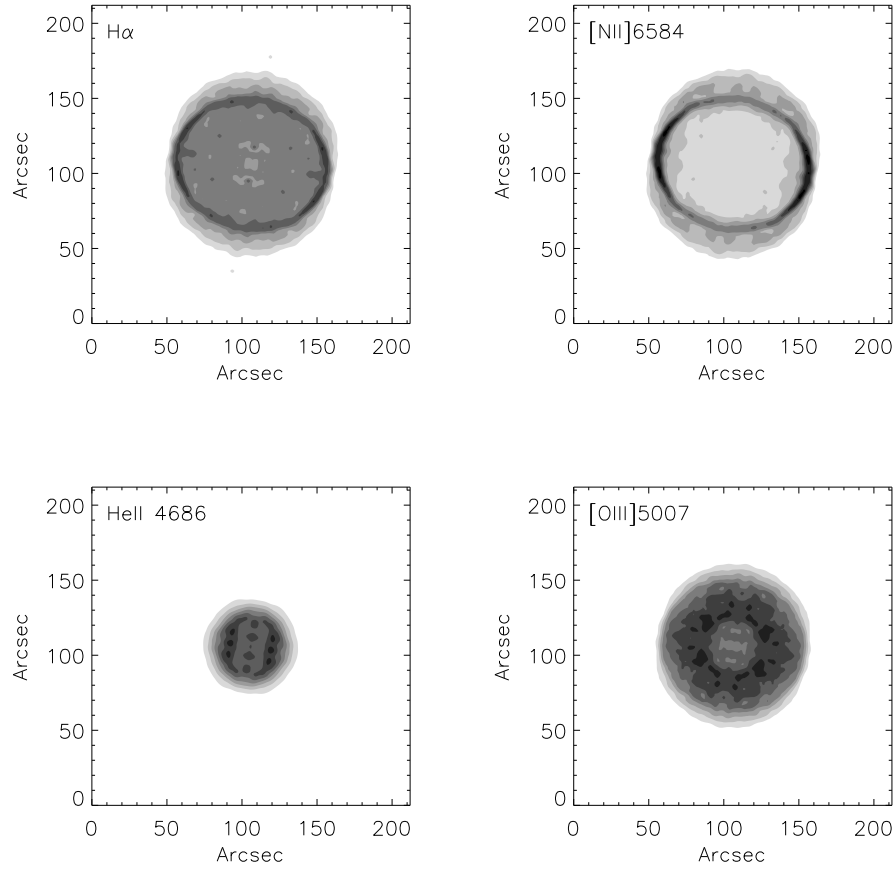


Fig. 4.— Images obtained from the projection at the observed angle of the data cubes of emissivities computed by the photoionization code for the most important emission lines. Compare these model images with the observed images in Mavromataki et al. (2001).

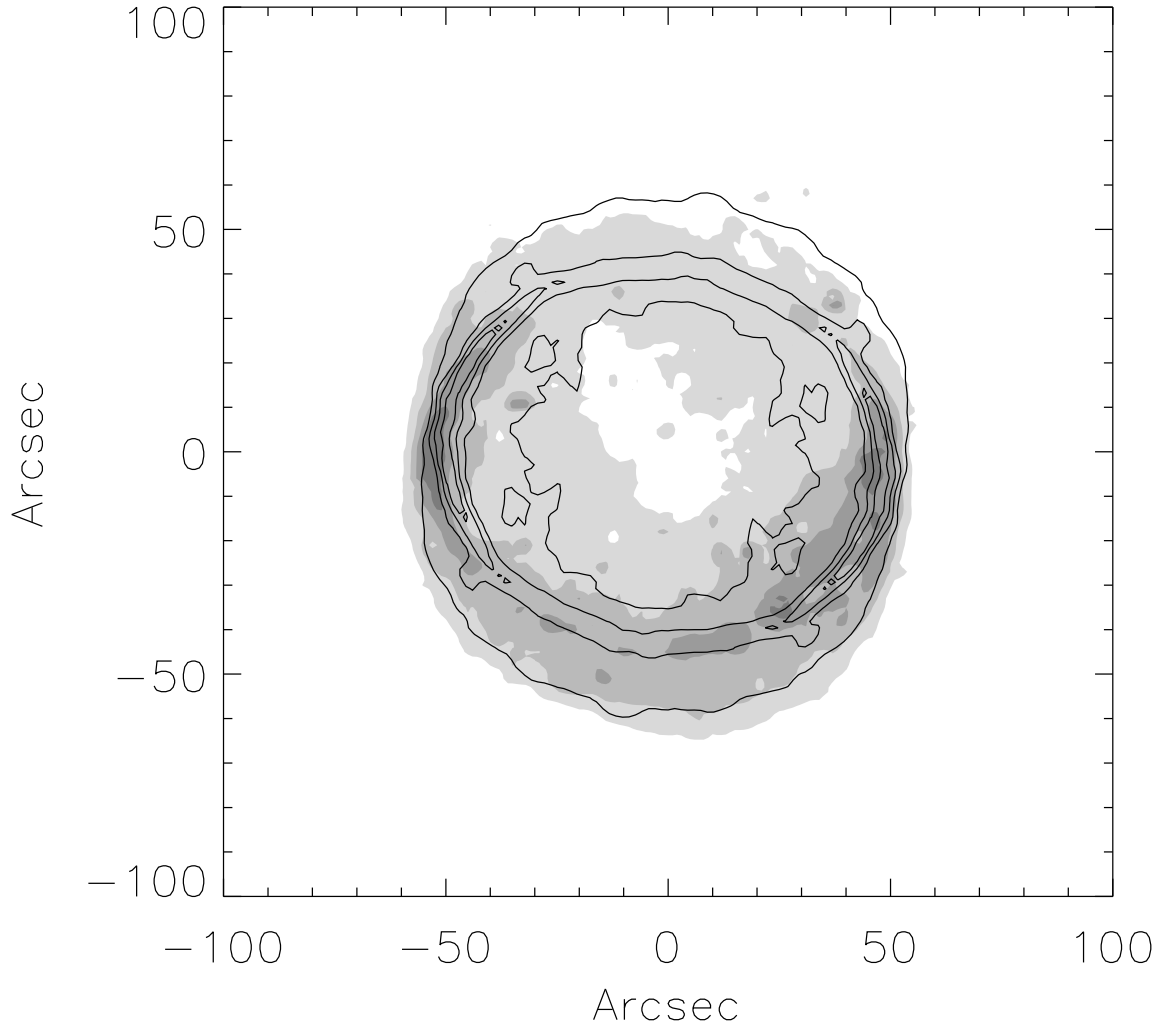


Fig. 5.— Image comparing the observed [NII]658.4 nm narrow band image with the contours of the equivalent image of the fitted model. Note the similarity between the observed and modeled images.

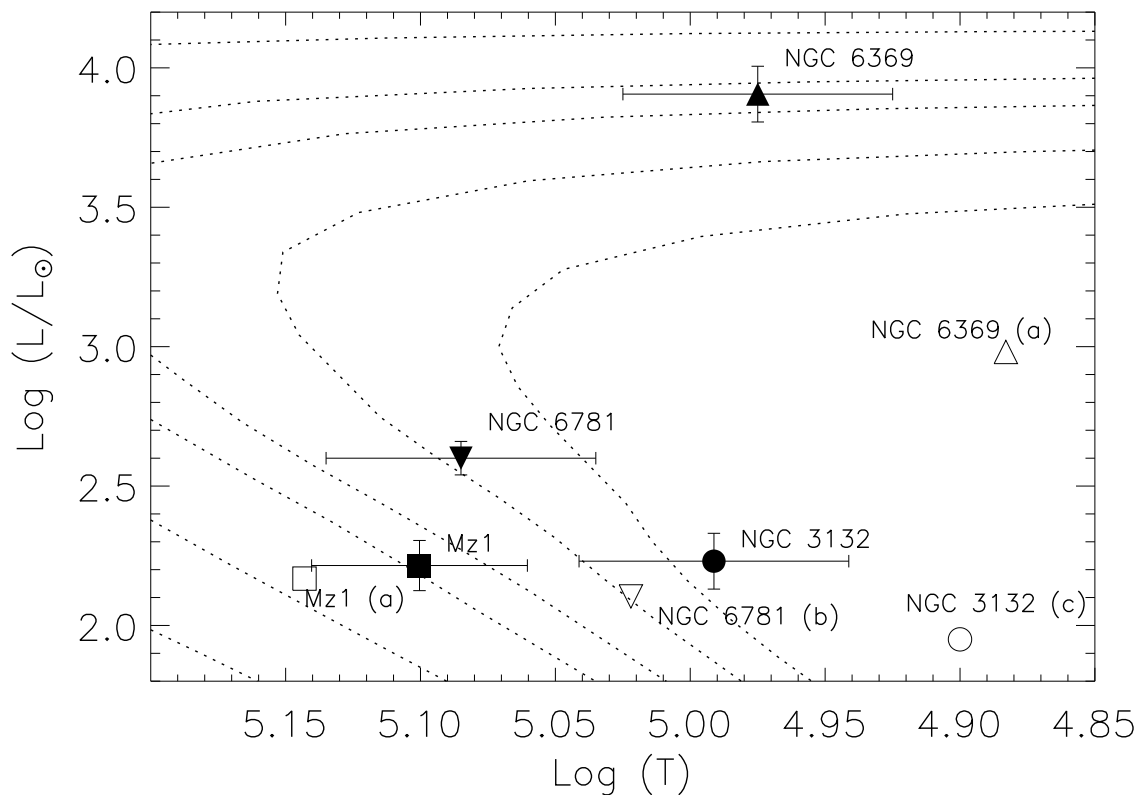


Fig. 6.— HR diagram for NGC 6781, NGC 3132 (Monteiro, Morisset, Gruenwald & Viegas (2000)), NGC 6369 (Monteiro, Schwarz, Gruenwald & Heathcote (2004)), MZ 1 (Monteiro, Schwarz, Gruenwald, Guenther & Heathcote (2005)), all PNe that had their central star properties determined by our method. Also plotted are the literature values for comparison. a) Stanghellini, Corradi & Schwarz (1993); b) Stanghellini, Villaver, Manchado & Guerrero (2002); c) . The evolutionary tracks are from Vassiliadis & Wood (1994); they are similar to the Blöcker (1995) models but take metallicities etc. into account. .

Table 2: Comparison of parameters found in the literature and those determined by our 3-D method.

Object	Our T	HeII/HI	[OIII]/[OII]	Our L(L _⊙)	Our d(pc)
Hb 5	230 ^a	131 ^b	-	6000 ^a	1400 ^a
Mz1	120 ^c	139 ^d	-	164 ^c	1050 ^c
NGC 3132	90 ^e	80 ^c	36 ^c	150 ^e	930 ^e
NGC 6369	91 ^f	122 ^g	60 ^g	8100 ^f	1550 ^f
NGC 6781	123 ^h	126 ^g	68 ^g	385 ^h	950 ^h

a) Preliminary results from Rice, Schwarz & Monteiro (2004) b) Kaler & Jacoby (1989) c) Phillips (2003) d) Monteiro, Schwarz, Gruenwald, Guenther & Heathcote (2005) e) Monteiro, Morisset, Gruenwald & Viegas (2000) f) Monteiro, Schwarz, Gruenwald & Heathcote (2004) g) Gurzadyan (1997) h) This paper.